

Broadband noise control based on the coupling of Bragg reflection and local resonance

Xu WANG¹; Wuzhou YU; Zaixiu JIANG; Xingyi ZHU; Dongxing MAO

Institute of Acoustics, Tongji University, No. 1239 Siping Road, Shanghai 200092, China

ABSTRACT

This paper presents a theoretical study of a duct loaded with identical side-branch resonators. The Bloch wave theory and the transfer matrix method are used to investigate wave propagation in the duct. The strong coupling effect resulted from both the Bragg reflection and local resonance is observed when the periodic distance and the resonators geometries are “matched”. Such a effect results in a broad noise attenuation band in low frequencies and may have a potential application in broad band noise control.

Keywords: Helmholtz resonators, Bragg reflection, Coupling effect

I-NCE Classification of Subjects Number(s): 51.1

1. INTRODUCTION

Helmholtz resonators (hereafter resonators) are devices with a resonance peak designed to control noise in a narrow frequency range.^{1,2} Given that a single resonator has a narrow resonance peak, combining several resonators is one possible way of obtaining a broader noise attenuation band.^{3,4} A duct loaded with identical resonators investigated by Sugimoto and Horioka is found to be a new class of ultrasonic metamaterial.^{5,6} Unlike previous theoretical discussions on the infinite periodic duct-resonator,^{5,6} the present study considers a duct with a finite number of identical resonators. A modified bandwidth approximation is then proposed. A duct loaded with identical resonators exhibits an unique attenuation characteristic, which has a potential application in broadband noise control.

2. THEORETICAL ANALYSIS

2.1 Single resonator

As shown in Fig. 1, resonators, with neck cross sectional area S_n , neck length l_n and cavity volume V_c , are mounted on a duct with cross sectional area S_d . Although the distributed-parameter model provides a more accurate prediction for the resonant frequency, only the lumped-parameter model is used here to give readers a clear and direct impression of the tendency of bandwidth to vary with the geometries of the resonators. Only the lossless case is considered. According to Ingard², the acoustic impedance of the resonator Z_r is given as

$$Z_r = j \frac{\rho_0 l_n'}{S_n \omega} (\omega^2 - \omega_0^2), \quad (1)$$

where ρ_0 is the air density, l_n' is the effective length of the neck, and ω_0 is the resonant circular frequency (i.e. $\omega_0 = c_0 \sqrt{S_n / l_n' V_c}$, c_0 the speed of sound in the air).

¹ xuwang@tongji.edu.cn

2.2 Multiple resonators

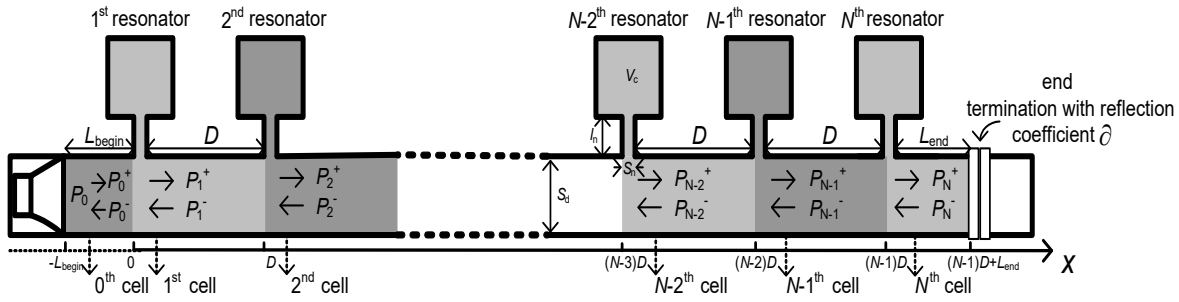


Figure 1 –A duct loaded periodically with N identical resonators.

As shown in Fig. 1, a typical periodic cell comprises a duct segment with a resonator attached to its left side. The diameter of the resonator neck is assumed to be negligible compared to the length of duct segment between two resonators, D . In other words, D can also be regarded as the periodic distance. The frequency range considered is well below the cut-on frequency of the duct. In the duct segment of the n^{th} cell for $(n-1)D \leq x \leq nD$, the sound traveling in positive- and negative- x directions can be described with sound pressure $P_n^+(x) = C_n^+ e^{-jk(x-(n-1)D)}$ and $P_n^-(x) = C_n^- e^{jk(x-(n-1)D)}$, where C_n^+ and C_n^- are complex constants and k is the wave number. Similarly, the sound pressure in the duct segment of the next cell can be expressed as $P_{n+1}^+(x) = C_{n+1}^+ e^{-jk(x-nD)}$ and $P_{n+1}^-(x) = C_{n+1}^- e^{jk(x-nD)}$. Combining the continuity of sound pressure and volume velocity at the point $x = nD$ yields

$$\begin{bmatrix} C_{n+1}^+ \\ C_{n+1}^- \end{bmatrix} = \begin{bmatrix} (1-\xi)e^{-jkD} & -\xi e^{jkD} \\ \xi e^{-jkD} & (1+\xi)e^{jkD} \end{bmatrix} \begin{bmatrix} C_n^+ \\ C_n^- \end{bmatrix} = \mathbf{T} \begin{bmatrix} C_n^+ \\ C_n^- \end{bmatrix} \quad (2)$$

where the 2×2 -dimensional matrix \mathbf{T} is the periodic transfer matrix. In Eq. (2), $\xi = Z_d / 2Z_r$, where

Z_d / Z_r is the acoustic impedance of the duct/resonator respectively, in which $Z_d = \rho_0 c_0 / S_d$.

According to the Bloch wave theory, Eq. (2) can also be expressed as

$$\begin{bmatrix} C_{n+1}^+ & C_{n+1}^- \end{bmatrix}^T = e^{-jqD} \begin{bmatrix} C_n^+ & C_n^- \end{bmatrix}^T \quad (3)$$

where the superscript T is the transposition and q is the Bloch wave number.¹⁰ Combining Eqs. (2) and (3), the analysis of a periodic duct-resonator system boils down to an eigenvalue problem that involves finding

the eigenvalue $\lambda = e^{-jqD}$ and the corresponding eigenvector $\mathbf{v} = [v^+ \quad v^-]^T$ for the transfer matrix \mathbf{T} .

Combining Eqs. (2) and (3) gives⁷

$$\cos(qD) = \cos(kD) + j\xi \sin(kD) \quad (4)$$

2.3 Coupling of the stopbands

Although Eq. (4) describes the frequency characteristics of the Bloch waves, it does not give an explicit expression about the position of the stop-bands, as well as their bandwidth. The theoretical prediction of the bandwidth has been proposed by Sugimoto and Horioka⁷ for small resonators (compared to geometries of the duct), and this paper will expand their work to a wider applicable range by adding some modification. In general, three types of stop-bands result from either the resonance of the resonators or the Bragg reflection, or from both.⁷ Using the definitions of Z_r and Z_d , Eq. (4) can be rewritten as

$$\cos(qD) = \cos(kD) + \frac{V_c k}{2S_d [(\omega/\omega_0)^2 - 1]} \sin(kD) \quad (5)$$

The first kind of stop-band (referred to as stop-band I) results from the resonance of the resonators. The stop-band is near ω_0 , as $\omega/\omega_0 = 1 + \Delta$, where $|\Delta| < 1$ is assumed. To differentiate it from the other two types of stop-bands, $k_0 D \neq m\pi$ here. When the modulus of Eq. (5) is equal to unity, the approximated stop-band boundary $\Delta_{1,2}$ can be obtained, as

$$\Delta_1 = \frac{V_c k_0}{4S_d} \cot\left[\frac{k_0 D}{2}(1 + \Delta_1)\right] = \frac{\kappa k_0 D}{4} \left[\cot\left(\frac{k_0 D}{2}\right) - \frac{1}{\sin^2(k_0 D/2)} \frac{k_0 D}{2} \Delta_1 + \dots \right] \quad (6)$$

$$\Delta_2 = -\frac{V_c k_0}{4S_d} \tan\left[\frac{k_0 D}{2}(1 + \Delta_1)\right] = -\frac{\kappa k_0 D}{4} \left[\tan\left(\frac{k_0 D}{2}\right) + \frac{1}{\cos^2(k_0 D/2)} \frac{k_0 D}{2} \Delta_2 + \dots \right] \quad (7)$$

where κ is the ratio of the cavity's volume to the duct's volume in a periodic cell ($\kappa = V_c / S_d D$), which is generally assumed to be smaller than unity ($\kappa < 1$). The terms in the square bracket of Eq. (6)/(7) are the series expansion of the cotangent/tangent terms, respectively. The zero order corrections (the first terms in the square brackets) of Eq. (6) and (7) give $\Delta_1 = \kappa k_0 D / 4 \cdot \cot(k_0 D / 2)$ and $\Delta_2 = -\kappa k_0 D / 4 \cdot \tan(k_0 D / 2)$, with a relative bandwidth $\Delta_{BW} = \kappa k_0 D / 2 \cdot |\tan(k_0 D / 2) + \cot(k_0 D / 2)|$. These are obtained from Sugimoto and Horioka's examination of the issue,⁷ and the bandwidth Δ_{BW} is of the order κ . However, this approximation has a significant deviation when $|\Delta| > 0.1$. A more accurate result can be obtained by considering the first order corrections (the second terms in the square brackets) of Eq. (6) and (7), or even the higher order corrections.

The second kind of stop-band (referred to as stop-band II) is the result of the Bragg reflection, which occurs when the periodic distance becomes a multiple of a half-wavelength of sound waves ($kD = m\pi$ $m = 1, 2, \dots$).⁷ The stop-band is near $\omega_m = m\pi\omega_0 / D$, as $\omega/\omega_m = 1 + \Delta$. To differentiate it from the third case, $\omega_m \neq \omega_0$ here. In the frequency range of stop-band II, Eq. (5) can be approximated as

$$\cos(qD) = \cos(m\pi + \Delta m\pi) + \frac{V_c m\pi(1 + \Delta)}{2DS_d [(\omega_m(1 + \Delta)/\omega_0)^2 - 1]} \sin(m\pi + \Delta m\pi) = (-1)^m \left\{ 1 + \frac{(m\pi)^2}{2} E \right\} \quad (8)$$

$$E = \frac{\kappa(1 + \Delta)}{((1 + \Delta)\omega_m / \omega_0)^2 - 1} \Delta - \Delta^2 \quad (9)$$

E can be approximated as $G\Delta - \Delta^2$, where $G = \kappa / [(\omega_m / \omega_0)^2 - 1]$, which gives $\Delta_1 = 0$ and $\Delta_2 = \kappa / [(\omega_m / \omega_0)^2 - 1]$ with the relative bandwidth $\Delta_{BW} = \kappa / |(\omega_m / \omega_0)^2 - 1|$. This is derived by Sugimoto and Horioka,⁷ and the bandwidth Δ_{BW} is of the order κ . For stop-bands II where $\omega_m < \omega_0$, there is $1 + \kappa / [(\omega_m / \omega_0)^2 - 1] \leq \omega / \omega_m \leq 1$; for others in higher frequency ranges where $\omega_m > \omega_0$, there is $1 \leq \omega / \omega_m \leq 1 + \kappa / [(\omega_m / \omega_0)^2 - 1]$. Similarly, the approximation made above has a significant deviation when $|\Delta| > 0.1$. A modified approximation can be obtained by rewriting Eq. (9) as

$$E = \frac{\kappa(1 + \Delta)\Delta}{2\gamma^2\Delta + \gamma^2 - 1} - \Delta^2 \tag{10}$$

where $\gamma = \omega_m / \omega_0$. In addition to $\Delta_1 = 0$, there are two other roots, as

$$\Delta_{2,3} = \frac{\kappa + 1 - \gamma^2 \pm \sqrt{(\gamma^2 - 1 - \kappa)^2 + 8\kappa\gamma^2}}{4\gamma^2} \tag{11}$$

For the stop-bands II of $\gamma < 1$, Δ_2 is in the range of $(-1, 0)$, which is the physically reasonable root. For the stop-bands II of $\gamma > 1$, the Δ_3 in the range of $(0, 1)$ should be selected.

The third case (referred to as stop-band III) results from both the resonance of the resonator and the Bragg reflection (i.e. $\omega_m = \omega_0$). In the frequency range of stop-band III, Eq. (9) can be approximated as

$$E = \kappa / 2 - \Delta^2, \text{ with } \Delta_{1,2} = \pm\sqrt{\kappa/2} \text{ and } \Delta_{BW} = \sqrt{2\kappa}. \text{ This is obtained from Sugimoto and}$$

Horioka,⁵ and the stop-band III is widened to be of the order $\sqrt{\kappa}$. As D is in this case limited to $m\pi / k_0$,

the relative bandwidth Δ_{BW} is at its maximum value when $m = 1$. Similarly, the approximation has a significant deviation when $|\Delta| > 0.1$. Substituting $\omega_m / \omega_0 = 1$ into Eq. (9) gives

$$\Delta^3 + 2\Delta^2 - \kappa\Delta - \kappa = 0 \tag{12}$$

The equation above has three roots, as

$$\Delta_1 = -\frac{2}{3} - \frac{2}{3}\sqrt{4 + 3\kappa} \cos\left(\frac{\theta}{3}\right) \tag{13}$$

$$\Delta_{2,3} = -\frac{2}{3} + \frac{\sqrt{4 + 3\kappa}}{3} \left[\cos\left(\frac{\theta}{3}\right) \pm \sqrt{3} \sin\left(\frac{\theta}{3}\right) \right] \tag{14}$$

where $\theta = \arccos(K)$, $K = (16 - 9\kappa) / [2(4 + 3\kappa)^{1.5}]$. As $\Delta_1 < -1$ is physically impossible, the other two roots $\Delta_{2,3}$ are chosen. Compared to the results obtained by Sugimoto and Horioka⁵, Eq. (14) indicates that f_0 is not exactly in the middle of the stop-band.

3. RESULTS AND DISCUSSIONS

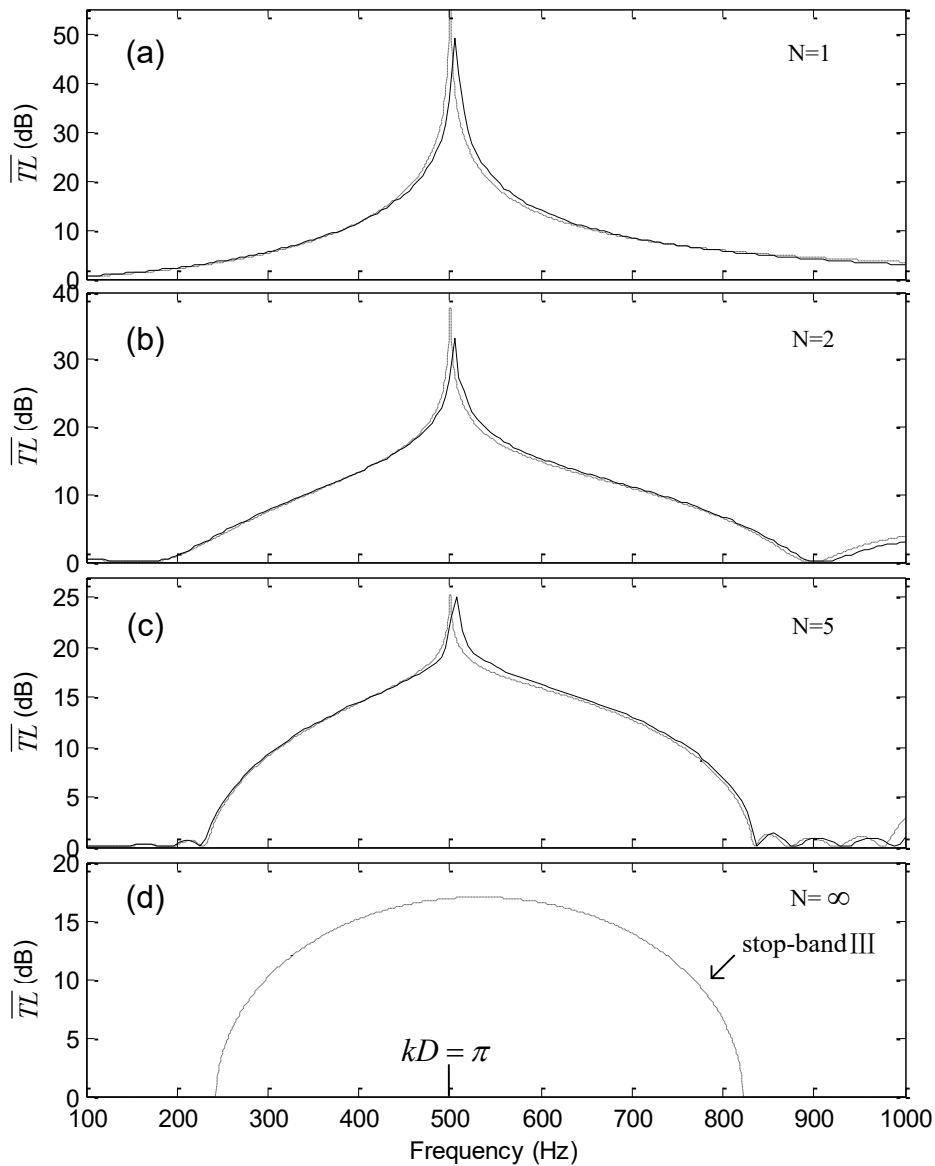


Figure 2 –The averaged transmission loss \overline{TL} of the duct with N resonators (the solid lines represent the FEM simulation and the dotted lines represent the theoretical prediction).

Fig. 2 show the averaged transmission loss, \overline{TL} of ducts with resonators ($N=1,2,5,\infty$). In Fig. 2, when the cases $N=1$ are compared to other cases, there is a clear impression of the difference caused by structural periodicity. The cases $N=2$, shown in Fig. 2(b), illustrate the rudiments of the frequency attenuation caused by structural periodicity; the original pattern of frequency attenuation begins to break down under the influence of the emerging structural periodicity. In the cases $N=5$, shown in Fig. 2(c), the width of the stop-bands decreases and a ripple pattern is observed beside them. That pattern disappears when $N=\infty$, as can be seen in Fig. 2(d). As shown in the figure, the strong coupling effect resulted from both the Bragg reflection and local resonance is observed when the periodic distance and the resonators geometries are “mathched”.

4. CONCLUSIONS

This paper has presented a theoretical study of a duct with identical resonators. The Bloch wave theory and the transfer matrix method are used to investigate wave propagation in the duct. The strong coupling effect resulted from both the Bragg reflection and local resonance is observed when the periodic distance and the resonators geometries are “matched”. Compared to a single resonator, a duct with several identical resonators exhibits a unique attenuation characteristic caused by structural periodicity, and may, if carefully designed, provide a much broader noise attenuation bands.

ACKNOWLEDGEMENTS

This work was financially supported in part by the National Natural Science Foundation of China under Grant Nos. 11304229, as well as the Fundamental Research Funds for the Central Universities.

REFERENCES

1. J. W. S. Rayleigh, *The Theory of Sound, Volume II* (Dover, New York, 1945), Chap. 16, pp. 303-322.
2. U. Ingard, “On the theory and design of acoustic resonators,” *J. Acoust. Soc. Am.* 25, 1037-1061(1953).
3. A. Trochidis, “Sound transmission in a duct with an array of lined resonators,” *J. Vib. Acoust.* 113, 245-249 (1991).
4. S. H. Seo and Y. H. Kim, “Silencer design by using array resonators for low-frequency band noise reduction,” *J. Acoust. Soc. Am.* 118(4), 2332-2338 (2005).
5. N. Sugimoto and T. Horioka, “Dispersion characteristics of sound waves in a tunnel with an array of Helmholtz resonators,” *J. Acoust. Soc. Am.* 97(3), 1446-1459 (1995).
6. N. Fang, D. J. Xi, J. Y. Xu, M. Ambati, W. Srituravanich, C. Sun, and X. Zhang, “Ultrasonic metamaterials with negative modulus,” *Nature Mater.* 5, 452-456 (2006).
7. D. C. Lay, *Linear Algebra and its Applications* (Addison Wesley, New York, 1994), Chap. 6, pp. 280-287.